

Thermal effects on the propagation of large-amplitude electromagnetic waves in magnetized relativistic electron-positron plasma

Macarena Domínguez,¹ Víctor Muñoz,¹ and Juan Alejandro Valdivia^{1,2}

¹*Departamento de Física, Facultad de Ciencias, Universidad de Chile, Santiago, Chile*

²*Centro para el Desarrollo de la Nanociencia y la Nanotecnología, CEDENNA, Chile*

(Received 29 March 2012; published 31 May 2012)

The propagation of circularly polarized electromagnetic waves along a constant background magnetic field in an electron-positron plasma is calculated by means of both a fluid and a kinetic theory treatment. In the fluid theory, relativistic effects are included in the particle motion, the wave field, and in the thermal motion by means of a function f , which depends only on the plasma temperature. In this work we analyze the consistency of the fluid results with those obtained from a kinetic treatment, based on the relativistic Vlasov equation. The corresponding kinetic dispersion relation is numerically studied for various temperatures, and results are compared with the fluid treatment. Analytic expressions for the Alfvén velocity are obtained for the fluid and kinetic models, and it is shown that, in the kinetic treatment, the Alfvén branch is suppressed for large temperatures.

DOI: [10.1103/PhysRevE.85.056416](https://doi.org/10.1103/PhysRevE.85.056416)

PACS number(s): 52.27.Ep, 52.27.Ny, 52.35.Mw

I. INTRODUCTION

The propagation of nonlinear waves in relativistic electron-positron plasmas has been a subject of interest for decades, due to their relevance in astrophysical environments, in connection with systems such as accretion disks [1], jet formation [2,3], early universe [4,5], and pulsar magnetospheres [6,7], and also in laboratory environments, where problems such as pair production by optical lasers [8,9] have been considered.

Recently, an exact solution in the context of fluid theory has been obtained for a circularly polarized wave propagating along a constant magnetic field in an electron-positron plasma with temperature [10]. Basing the approach on the magnetofluid field unification formalism [11], it can be shown that relativistic thermal effects can be consistently included by means of a function f , which depends only on the plasma temperature. The formalism in Ref. [11] has also been successfully used to study wave propagation in relativistic two-fluid plasmas [12], to find equilibrium states via a variational principle [13], and has been extended to non-Abelian fields in order to study quark-gluon plasmas [14]. In Ref. [10], the dispersion relation of large amplitude circularly polarized waves was derived, and its temperature dependence was studied numerically. In the nonrelativistic treatment, two branches exist: an electromagnetic one, which propagates for frequencies above the plasma frequency, and an Alfvén branch, which propagates for frequencies below the cyclotron frequency. Relativistic thermal effects produce: (a) a decrease of the effective plasma frequency (thus, waves in the electromagnetic branch can propagate for lower frequencies than in the cold case); and (b) a decrease of the upper frequency cutoff for the Alfvén branch (thus, Alfvén waves are confined to a frequency range which is narrower than in the cold case).

These results have been found in the context of a fluid model. However, effects such as Landau and cyclotron damping are absent in such a model, and thus it would be interesting to study to what extent the fluid results are modified by kinetic effects. Many works have been devoted to the study of kinetic effects on wave propagation in relativistic electron positron plasmas, either in the absence of magnetic field [15,16], to analyze the counterstreaming plasmas in pulsar

environments [17], to study the effect of nonlinearities and wave damping [18], to model the propagation of Bernstein waves [19], etc.

In this work, our aim is to study the propagation of a large amplitude circularly polarized electromagnetic wave in a magnetized plasma, analyzing the consistency of the results obtained in Ref. [10] and mentioned above, with those obtained from a kinetic treatment [20]. In effect, the same system is studied, but starting from the relativistic Vlasov equation. The corresponding kinetic dispersion relation is numerically studied for various temperatures, and results are compared with the purely fluid treatment. In our treatment, we assume that kinetic effects are only important along the propagation direction, which makes it necessary to generalize the fluid dispersion relation, already found in Ref. [10], but in the presence of drift.

The paper is organized as follows. In order to gain intuition for developing the posterior kinetic analysis, in Sec. II, the fluid relativistic dispersion relation of a circularly polarized electromagnetic wave propagating along a constant background magnetic field in an electron-positron plasma is solved. This corresponds to a generalization of the numerical results shown in Ref. [10], for the case of a plasma with constant longitudinal drift velocity. Then, the basic equations of the kinetic model are presented in Sec. III. In Sec. IV the dispersion relation of this wave is calculated. Then, in Sec. V the kinetic dispersion relation obtained in Sec. IV is solved numerically, and results are compared with the corresponding fluid treatment. Finally, in Sec. VI, results are summarized and discussed.

II. FLUID DISPERSION RELATION

In Ref. [10], the exact dispersion relation of a circularly polarized transverse electromagnetic wave, propagating along a constant background magnetic field, is found. Relativistic thermal effects were consistently included in a fluid model by means of a function f , which depends only on the plasma temperature. Using the magnetofluid field unification formalism and assuming thermal equilibrium ($f_e = f_p = f$),

the following dispersion relation is obtained [10]:

$$0 = k^2 c^2 - \omega^2 + \omega_p^2 \sum_j \left(\frac{\omega'}{f \omega' \gamma_j - \Omega_{cj}} \right), \quad f = \frac{K_3(\mu)}{K_2(\mu)}, \quad (1)$$

where $\omega' = \omega - v_z k$, v_z is a drift velocity along the background magnetic field, Ω_{cj} is the cyclotron frequency of species j ($j = p$ for positrons, and $j = e$ for electrons), ω_p is the plasma frequency in laboratory frame, γ_j is the relativistic Lorentz factor for species j , $K_n(\mu)$ is the modified Bessel function of order n , $\mu = mc^2/(k_B T)$, and k_B is the Boltzmann constant. Notice that the drift velocity is assumed to be the same for both species, so that there is no current in the absence of the wave.

Defining normalized variables $x = \omega/\Omega_{cp}$, $y = ck/\Omega_{cp}$, and $\beta = p_z/(mc)$, Eq. (1) can be written in normalized form as:

$$0 = y^2 - x^2 + \frac{\omega_p^2}{\Omega_{cp}^2} \sum_{j=p,e} \frac{x\gamma_j - y\beta}{f(x\gamma_j - y\beta) - \chi_j \gamma_j}, \quad (2)$$

where χ_j is the sign of the charge of species j , so that $\chi_p = 1$ and $\chi_e = -1$.

In order to solve the fluid dispersion relation given by Eq. (2), the roots of the following quartic equation for γ_j must be found:

$$\begin{aligned} 0 = & \gamma_j^4 f^2 - \gamma_j^3 \frac{2f}{x} (y\beta f + \chi_j) \\ & + \gamma_j^2 \left[\frac{(y\beta f + \chi_j)^2}{x^2} - (1 + \beta^2) f^2 - \alpha^2 \right] \\ & + \gamma_j \frac{2}{x} [(1 + \beta^2) f (y\beta f + \chi_j) + y\beta \alpha^2] \\ & - \frac{1}{x^2} (1 + \beta^2) (y\beta + \chi_j)^2 + y^2 \beta^2 \alpha^2, \end{aligned} \quad (3)$$

where

$$\alpha = \frac{e|A|}{mc^2} = \frac{e|E|}{mc\omega} = \frac{e|B|}{mc^2 k}. \quad (4)$$

Here \vec{A} , \vec{E} , and \vec{B} are the vector potential, electric field, and magnetic field of the wave, respectively.

Equation (3) is the generalization of Eq. (15) in Ref. [20] for $f \neq 1$ and $\beta \neq 0$. In Ref. [10] the case $f = 1$ was solved. We now consider the general case given by Eq. (3), to solve the dispersion relation given by Eq. (2) for both nonzero temperatures ($f \neq 1$) and nonzero drift velocities ($\beta \neq 0$).

To do this, we first choose fixed values for y , β , f , and α and a trial value for x . Equation (3) is then solved for γ_p and γ_e . Only solutions $\gamma_j \geq 1$ are physically acceptable. This yields several possible pairs (γ_p, γ_e) . Each possible pair corresponds to a different branch of the dispersion relation. When a pair is chosen, then the right-hand side of Eq. (2) can be evaluated. However, it turns out that, in general, the number of acceptable solutions of Eq. (3) for γ_e and γ_p is greater than 2, and this number changes for each value of β . This issue complicates the choice of γ_j .

This is illustrated in Fig. 1. For given values of y , α , and f , we solve Eq. (3) for a certain value of x and β , obtaining four roots, $\gamma_j^{(s)}$. We sort them such that $\text{Re}\gamma_j^{(1)} \leq \text{Re}\gamma_j^{(2)} \leq$

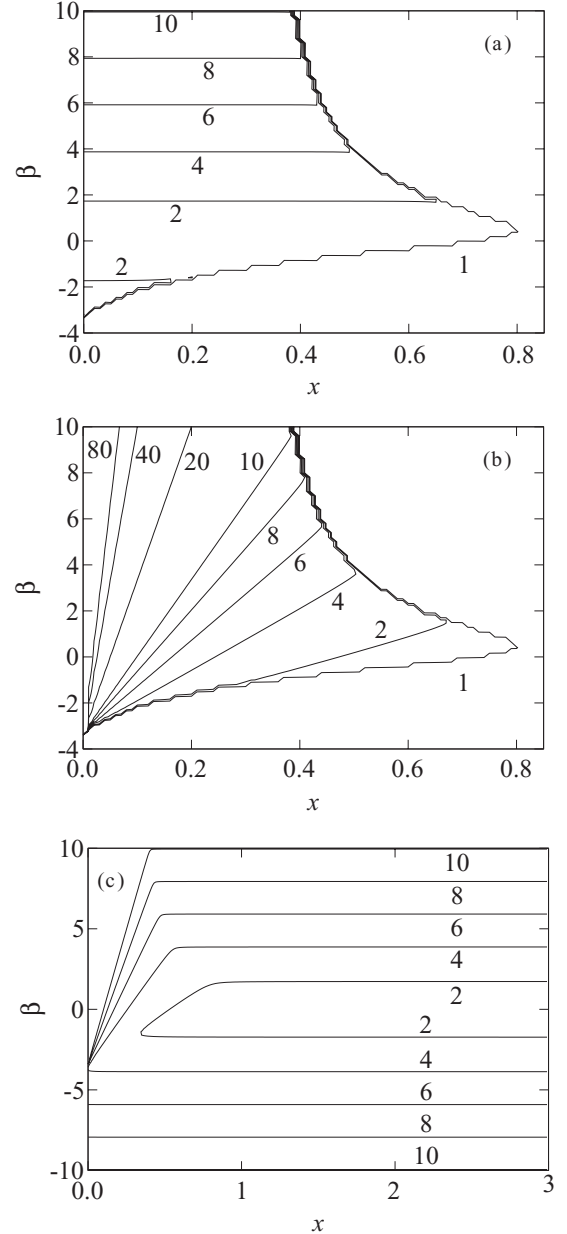


FIG. 1. Isocontours of real solutions of Eq. (3) as a function of normalized drift β and normalized frequency x for positrons. Each panel corresponds to a different branch, $\gamma_p^{(s)}$, for the roots of Eq. (3). A few contour levels are shown. Physically acceptable solutions are in the regions where $\gamma(x, \beta)$ is real and greater than 1. Fixed values $y = 0.3$, $\alpha = 0.1$, and $f = 1$ were taken. (a) $s = 1$, (b) $s = 2$, and (c) $s = 3$.

$\text{Re}\gamma_j^{(3)} \leq \text{Re}\gamma_j^{(4)}$. Figure 1 shows, for a certain range of values of x and β , the regions where the s th branch for positrons, $\gamma_p^{(s)}$, is physically acceptable, that is, real and greater than 1.

Figure 1 shows that for $x > 0.8$, approximately, there is only one possible choice, $\gamma_p^{(3)}$. However, for lower values of the frequency, there is a range of values of β where more than one choice of γ_p is possible. For instance, for $x = 0.400087$, $y = 0.3$, and $\beta = 4.4$, the three possible values are $\gamma_p^{(1)} = 4.12392$, $\gamma_p^{(2)} = 5.72992$, and $\gamma_p^{(3)} = 5.86722$.

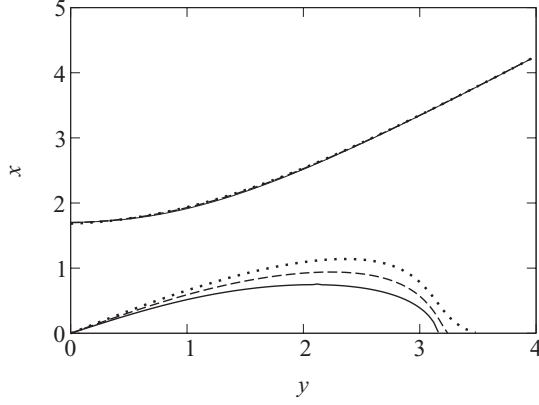


FIG. 2. Solutions of the dispersion relation Eq. (1) for $f = 1$, $\alpha = 0.1$, $v_{A0} = 1$ [see Eq. (6) below], and three values of β : $\beta = 0$ (solid line), $\beta = 0.1$ (dashed line), $\beta = 0.2$ (dotted line).

With a similar analysis in the case of γ_e , now we choose one of the possible branches for γ_p and one of the branches for γ_e , and we can calculate the right-hand side of Eq. (2) by solving for the value of x for which it is zero. Notice that it could still be the case that a chosen pair (γ_p, γ_e) yields an Eq. (2) with no real solutions for x . It turns out that there is only one choice of the (γ_e, γ_p) pair for which a real root of Eq. (2) can be found.

In Fig. 2 we plot the solutions of the dispersion relation (2), obtained by the method outlined above. The solid line, $\beta = 0$, corresponds to the solution already found in Ref. [10], which shows that our treatment leads to the correct limit in the absence of drift.

Notice that the Alfvén branch is much more sensitive to variations in drift than the electromagnetic branch. For small values of the frequency, it follows the usual linear dispersion relation, $\omega \simeq v_A k$, with v_A the Alfvén speed. v_A can be calculated by noting that, in this region, $\gamma_{\perp p}, \gamma_{\perp e} \sim 1 + \beta^2$, and by setting $\omega \ll \Omega_c$ in Eq. (1). This yields

$$\frac{v_A}{c} = \frac{2f\beta\sqrt{1+\beta^2} + v_{A0}\sqrt{(1+\beta^2)v_{A0}^2 + 2f\sqrt{1+\beta^2}}}{v_{A0}^2\sqrt{1+\beta^2} + 2f(1+\beta^2)}, \quad (5)$$

where

$$v_{A0} = \frac{\Omega_{cp}}{\omega_p} \quad (6)$$

is the normalized Alfvén velocity in the nonrelativistic cold fluid case.

For $\beta = 0$ the result in Ref. [10] is recovered, namely $v_A/c = v_{A0}/\sqrt{v_{A0}^2 + 2f}$. In Fig. 3 we plot the Alfvén velocity. In principle, v_A depends both on the drift velocity and the temperature. For illustration purposes, in Fig. 3 we have first taken a fixed temperature [Fig. 3(a)] and then a fixed drift velocity [Fig. 3(b)]. Qualitatively, similar results are obtained for other choices of f and β . What is important to notice is that the drift velocity and the temperature have the opposite effect on the Alfvén speed: v_A increases with β and decreases with f .

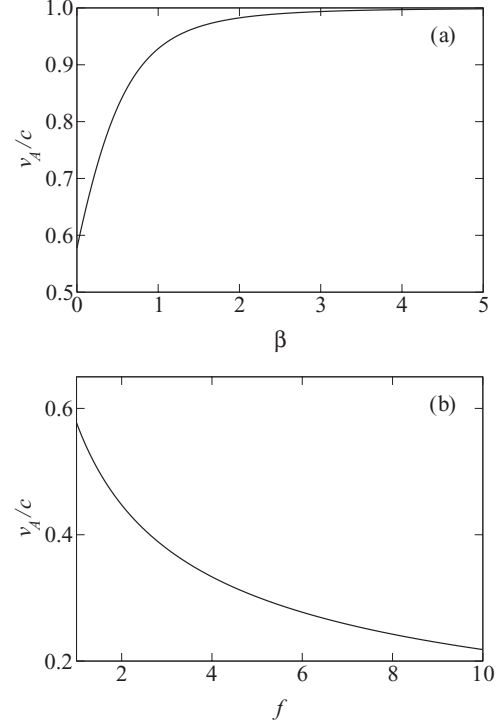


FIG. 3. Alfvén velocity [Eq. (5)] for $\alpha = 0.1$, $v_{A0} = 1$. (a) For fixed temperature, $f = 1$, as a function of the drift velocity β . (b) For fixed drift velocity, $\beta = 0$, as a function of temperature, parameterized by f .

III. KINETIC MODEL

In our treatment, we consider kinetic effects only along a background magnetic field $B_{0z}\hat{z}$ and a cold fluid model in the perpendicular direction [15,21].

The electromagnetic fields are described by Maxwell equations and the wave equation,

$$\left(\nabla^2 - \frac{1}{c^2} \frac{\partial^2}{\partial t^2}\right) \vec{A} = -\frac{4\pi}{c} \vec{J}_t, \quad (7)$$

where \vec{J}_t is the transverse current, with respect to the background magnetic field.

In order to describe the plasma, for the transverse fluid equations, we have

$$\left(\frac{\partial}{\partial t} + \vec{v}_j \cdot \vec{\nabla}\right) (\gamma \vec{v}_j) = \frac{q_j}{m_j} \left(\vec{E} + \frac{1}{c} \vec{v}_j \times \vec{B}\right), \quad (8)$$

$$\frac{\partial n_j}{\partial t} = -\vec{\nabla} \cdot (n_j \vec{v}_j),$$

where \vec{v}_j , q_j , m_j , and n_j are the velocity, charge, mass, and density of species j , respectively. On the other hand, the transverse current is given by

$$\vec{J}_t = \sum_j q_j n_j \vec{v}_{jt}, \quad (9)$$

where \vec{v}_{jt} is the transverse velocity of species j .

For the longitudinal direction, we consider the one-dimensional Vlasov equation:

$$\frac{\partial g_j}{\partial t} + \vec{v} \cdot \vec{\nabla} g_j + \frac{q_j}{m_j} \left(\vec{E} + \frac{1}{c} \vec{v} \times \vec{B} \right) \cdot \vec{\nabla}_{\vec{v}} g_j = 0, \quad (10)$$

where g_j is the velocity distribution function for species j , normalized so that

$$\int d\vec{v} g_j(\vec{r}, \vec{v}, t) = n_{j0},$$

with n_{j0} as the equilibrium unperturbed density for species j , and Poisson equation

$$\nabla^2 \varphi = -4\pi \sum_j q_j n_j. \quad (11)$$

Thus, the total density and transverse current are given by

$$n_j = \sum_j \int d\vec{v} g_j(\vec{r}, \vec{v}, t), \quad (12)$$

$$\vec{J}_t = \sum_j q_j \int d\vec{v} g_j(\vec{r}, \vec{v}, t) \vec{v}_{jt}, \quad (13)$$

respectively.

IV. DISPERSION RELATION

We now consider an electromagnetic wave propagating in the electron-positron plasma. In the absence of the wave, the plasma is considered to have no electric field, a uniform background magnetic field $\vec{B}_0 = B_0 \hat{z}$, equal densities for each species ($n_{e0} = n_{p0} = n_0$), and equal drifts for each species ($\vec{v}_{j0} = v_{z0} \hat{z}$).

We consider a circularly polarized wave that propagates along the \hat{z} axis, whose electric and magnetic fields are given by

$$\vec{E}_1(z, t) = E_1 [\sin(kz - \omega t) \hat{x} - \cos(kz - \omega t) \hat{y}], \quad (14)$$

$$\vec{B}_1(z, t) = \bar{B}_1 [\cos(kz - \omega t) \hat{x} + \sin(kz - \omega t) \hat{y}], \quad (15)$$

respectively.

If we define transverse quantities as

$$C_{\perp} = C_x + iC_y, \quad (16)$$

then Maxwell and Vlasov equations yield

$$\left(\nabla^2 - \frac{1}{c^2} \frac{\partial^2}{\partial t^2} \right) A_{\perp} = -\frac{4\pi}{mc} \sum_j q_j \int d\vec{p} v_{j\perp} g_j(\vec{x}, \vec{v}, t). \quad (17)$$

On the other hand, in order to introduce kinetic effects, we consider the following form of the distribution function:

$$g_j = n_0 \tilde{g}_j(z, p_z, t) \delta(p_x - p_x^f) \delta(p_y - p_y^f), \quad (18)$$

where \vec{p}^f is the transverse particle momentum obtained with the cold fluid theory. In the absence of the wave, the adimensional distribution function in Eq. (18) must satisfy $\tilde{g}_{e0} = \tilde{g}_{p0}$, so that densities are equal.

Then, Eq. (17) can be written in the form

$$\left(\nabla^2 - \frac{1}{c^2} \frac{\partial^2}{\partial t^2} \right) A_{\perp} = -\frac{4\pi n_0}{mc} \sum_j q_j \int dp_{\perp} v_{j\perp} \tilde{g}_j(z, p_z, t). \quad (19)$$

Note that we need to know $v_{j\perp}$ in order to be able to solve the dispersion relation. To do this, we consider that in the direction perpendicular to the magnetic field, the equations governing the system are the fluid equations.

In the presence of the wave, the velocity, magnetic field, and electric field are given by $\vec{v}_j = \vec{v}_{j0} + \vec{v}_{j1}$, $\vec{B} = \vec{B}_0 + \vec{B}_1$, and $\vec{E} = \vec{E}_1$, respectively. Using this in Eq. (8), we obtain

$$\begin{aligned} & \gamma \partial_t v_{j1x} + \gamma (v_{j0z} \partial_z v_{j1x} + v_{j1z} \partial_z v_{j1x}) \\ &= \frac{q_j}{m_j} \left[E_{1x} - \frac{B_{1y}}{c} (v_{j0z} + v_{j1z}) + \frac{v_{j1y} B_0}{c} \right], \end{aligned} \quad (20)$$

$$\begin{aligned} & \gamma \partial_t v_{j1y} + \gamma (v_{j0z} \partial_z v_{j1y} + v_{j1z} \partial_z v_{j1y}) \\ &= \frac{q_j}{m_j} \left[E_{1y} + \frac{B_{1x}}{c} (v_{j0z} + v_{j1z}) - \frac{v_{j1x} B_0}{c} \right], \end{aligned} \quad (21)$$

$$\begin{aligned} & \gamma \partial_t v_{j1z} + \gamma (v_{j0z} \partial_z v_{j1z} + v_{j1z} \partial_z v_{j1z}) \\ &= \frac{q_j}{m_j} \left[\frac{v_{j1x} B_{1y}}{c} - \frac{v_{j1y} B_{1x}}{c} \right]. \end{aligned} \quad (22)$$

Using Eq. (16), and assuming a time dependence for transverse quantities of the form $C_{\perp 1} = C e^{i(kz - \omega t)}$, then it can be shown that [10]

$$v_j = -\frac{q_j A}{m_j c k} \frac{\omega'}{\omega' \gamma_j - \Omega_{cj}}. \quad (23)$$

Finally, using Eq. (23) in Eq. (19), the following dispersion relation is obtained:

$$0 = k^2 c^2 - \omega^2 + \omega_p^2 \sum_j \int dp_z \frac{\omega'}{\omega' \gamma_j - \Omega_{cj}} \tilde{g}_{j0}. \quad (24)$$

V. NUMERICAL SOLUTION OF THE KINETIC DISPERSION RELATION

We now solve the kinetic dispersion relation Eq. (24). First, it is convenient to write it in normalized form:

$$y^2 - x^2 + \frac{\omega_p^2}{\Omega_{cp}^2} \sum_{j=p,e} \int d\beta \frac{x\gamma_j - \beta y}{x\gamma_j - \beta y - \chi_j} \frac{\tilde{g}_{j0}}{\gamma_j} = 0. \quad (25)$$

There are two main issues to consider at this point. One is the choice of the distribution function and the other is the choice of γ_j .

Regarding the distribution function, since we are interested in comparing the kinetic dispersion relation with the results in Ref. [10], which include the effects of relativistic temperature, we take $\tilde{g}_{p0} = \tilde{g}_{e0} \equiv \tilde{g}_0$ as a Maxwell-Boltzmann-Jüttner distribution:

$$\tilde{g}_0(\beta, \mu) = \frac{1}{2mc K_1(\mu)} e^{-\mu(1+\beta^2)^{1/2}}.$$

Thus, in the kinetic treatment, thermal information is contained in the normalized inverse temperature parameter μ . In the

fluid treatment described in Ref. [10], thermal information is contained in the parameter f .

Once the distribution function is chosen, the numerical strategy is analogous to the one outlined in Sec. II, except that an integration along the β axis must be done. This means that, for each trial frequency, the corresponding values of $\gamma(\beta)$ must be found. Since, in the transverse direction, we consider a cold fluid model, the problem of finding γ is equivalent to the one discussed in Sec. II for a cold fluid with a given longitudinal drift β . Thus, the equation to solve in order to find γ is Eq. (3), with $f = 1$. It must be solved for each point in the β axis, and once the integration is complete, the right-hand side of Eq. (24) can be evaluated. Thus, rather than finding a value of, say, γ_e to generate the electromagnetic branch in the fluid dispersion relation, the proper infinite set of values $\gamma_e(\beta)$ must be found.

If only two physically acceptable values of γ_j were obtained for each value of β then the problem would still be easy, since one of them would correspond to the electromagnetic branch and the other to the Alfvén branch, and there would be no ambiguity in the calculation of the integral. However, as shown in Sec. II, several values of γ_j are possible, both for electrons and positrons. Moreover, the problem is now more complicated, since in the kinetic case, there is an integral over β , thus a choice of branches for γ_j must be done at each point of the integration path. And since the number of valid values of γ_j changes with β (see Fig. 1), there is no guarantee that a choice for a given β is valid along the complete integration path. In fact, we have found that this is not the case, in general. By studying several families of parameters, we concluded that it is very difficult to find a general, reliable algorithm to automate the choice, and some trial and error is still involved in the results presented here.

The rest of the numerical procedure is equivalent to the fluid case: once a proper choice of $\gamma_j(x, \beta)$ is made, it is used to find a value of x such that Eq. (25) is satisfied, and the process is repeated for a different value of x .

Figure 4 shows the solution of the dispersion relation Eq. (1) for three different temperatures. This figure should be compared with Fig. 1 in Ref. [10], where three temperatures corresponding to $f = 1, 2$, and 10 were considered.

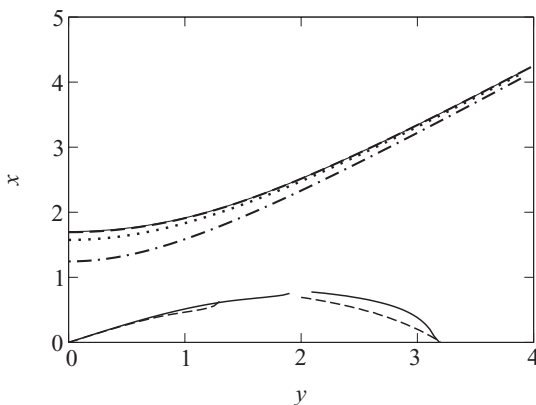


FIG. 4. Solutions of the dispersion relation Eq. (24) for $\alpha = 0.1$ and $v_{A0} = 1$. Solid line $\mu = 700$ ($f \simeq 1$); dashed line $\mu = 50$ ($f \simeq 1.1$); dotted line $\mu = 3$ ($f \simeq 2$); dot dashed line $\mu = 0.4$ ($f \simeq 10$).

We should first notice that, in the Alfvén branch, which starts at the origin, there is a small frequency region where no modes are found (in this case $y \sim 2$). This is a result of the technical issues regarding the choice of γ_j at each point of the integration path and illustrated in Fig. 1. On the other hand, the electromagnetic branch (for all wave numbers), and the Alfvén branch near the origin (for small values of $x = \omega/\Omega_{cp}$ and $y = ck/\Omega_{cp}$) can always be obtained without ambiguities in the choice of γ_j .

Thus, we will focus the remaining of the discussion on the electromagnetic branch and the region of the Alfvén branch near the origin. Solving the numerical issues near the maximum frequency in the Alfvén branch may involve either improving the numerical algorithms or improving on the cold model for the transverse motion [Eq. (18)], and we plan to deal with this problem elsewhere.

The first result to notice is that, indeed, the same branches as in the fluid case are found, an electromagnetic and an Alfvén branch. For very low temperatures, the cold result is recovered (see solid line in Fig. 2). When the temperature is increased (μ decreases), it is observed that the effect of the temperature is to decrease the effective plasma frequency and to decrease the upper frequency cutoff for the Alfvén branch. It is interesting to observe that this is qualitatively equivalent to what is obtained in the fluid theory.

However, several quantitative differences are found. First, in the kinetic model, the effective plasma frequency is less sensitive to variations in temperature than in the fluid model. This is shown in Fig. 5, where ω_p^{eff} [solution of the electromagnetic branch, Eq. (25) with $y = 0$] is plotted as a function of inverse normalized temperature μ , for both models. For any given temperature, the plasma frequency is always higher in the kinetic case than in the fluid case.

Regarding the Alfvén branch, analytical results can be obtained from Eq. (24), which is consistent with the numerical procedures that yield Fig. 4. Taking $\omega \ll \Omega_c$ in Eq. (24) yields the Alfvén velocity

$$\frac{v_A}{c} = \sqrt{\frac{v_{A0}^2 - I_1(\mu)}{v_{A0}^2 + I_2(\mu)}}, \quad (26)$$

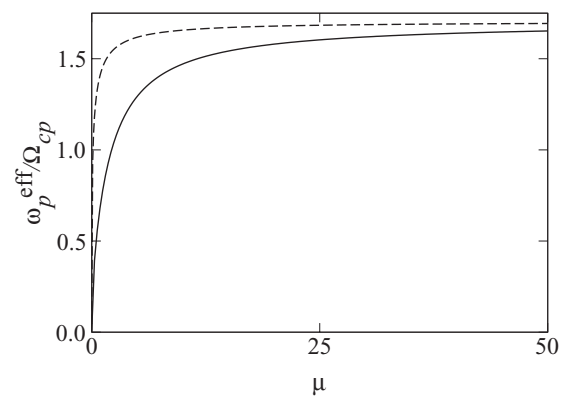


FIG. 5. Effective plasma frequency as a function of inverse normalized temperature μ . Solid line: fluid model. Dashed line: kinetic model.

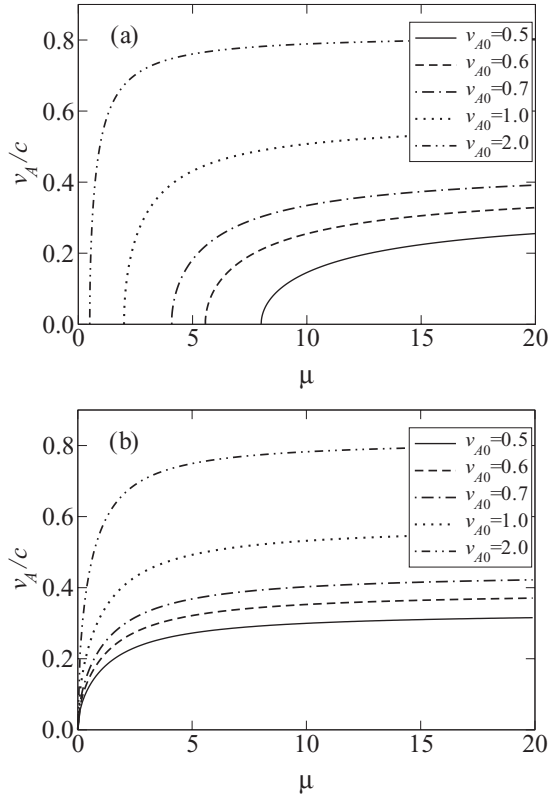


FIG. 6. Alfvén speed as a function of inverse normalized temperature μ . (a) Eq. (26) and (b) Eq. (5) ($\beta = 0$), for various values of v_{A0} .

where

$$I_1(\mu) = 2 \int d\beta \frac{\tilde{g}_0(\beta, \mu) \beta^2}{\sqrt{1 + \beta^2}}, \quad (27)$$

$$I_2(\mu) = 2 \int d\beta \tilde{g}_0(\beta, \mu) \sqrt{1 + \beta^2}. \quad (28)$$

The kinetic result, Eq. (26), as well as the fluid result, Eq. (15) in Ref. [10], are plotted as a function of μ in Fig. 6, for various selected values of v_{A0} .

We notice that increasing the temperature has the effect of decreasing the Alfvén speed [Fig. 6(a)]. The same qualitative behavior occurs in the fluid case [Fig. 6(b)]. However, in the

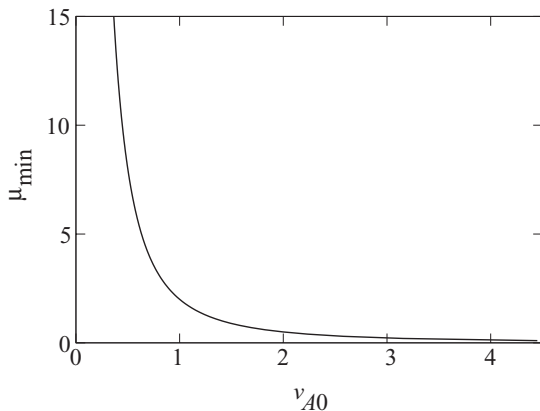


FIG. 7. Minimum value of μ as a function of v_{A0} .

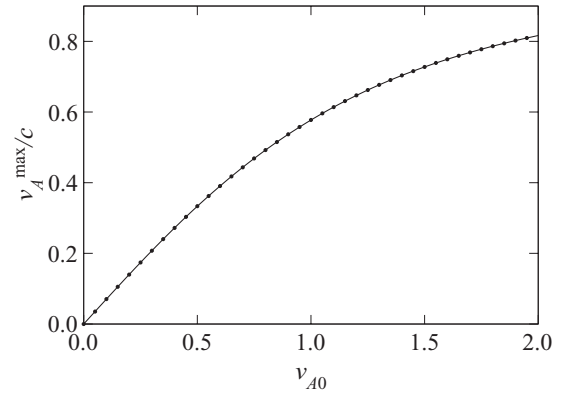


FIG. 8. Maximum Alfvén speed as a function of v_{A0} , obtained from solving the kinetic dispersion relation Eq. (24) for very low temperature (solid line) and from the fluid model, Eq. (15) in Ref. [10] (dotted).

kinetic treatment, unlike the fluid case, the Alfvén branch is suppressed for large temperatures. The threshold temperature (proportional to μ^{-1}), below which the Alfvén branch exists, is larger if v_{A0} increases. That is, if, say, the density is constant, the Alfvén branch exists for a larger range of temperatures when the background magnetic field is increased. The threshold can be obtained from Eq. (26) by noting that it satisfies

$$v_{A0}^2 - I_1(\mu_{\min}) = 0. \quad (29)$$

Figure 7 shows the value of μ_{\min} for various values of v_{A0} . If the density is fixed, Fig. 7 shows that Alfvén waves can propagate for larger values of the temperature (μ_{\min} is smaller) if the background magnetic field is increased (v_{A0} increases).

Figure 6 also shows that, for a given value of v_{A0} (fixed amplitude of the background magnetic field, for instance), the maximum Alfvén speed is obtained in the cold limit.

The result obtained in Eq. (26) is fully consistent with the fluid model in the cold limit. In fact, if $\mu \rightarrow \infty$ in Eqs. (27) and (28), then $I_1 \rightarrow 0$ and $I_2 \rightarrow 2$, thus recovering the result obtained in Eq. (15) of Ref. [10].

In Fig. 8 we plot the maximum value of the Alfvén speed as a function of v_{A0} as given by the kinetic model [Eq. (26) with a very large value of μ] and by the fluid model [Eq. (15) in Ref. [10], with $f = 1$].

The fact that both results match shows that, in spite of the technical issues discussed above regarding the proper choice of γ at each point in the integration path, the kinetic model presented here still yields the fluid result in the proper limit.

VI. SUMMARY

In this paper, we have studied the propagation of a large amplitude circularly polarized electromagnetic wave along a constant magnetic field in a relativistic electron-positron plasma. The plasma is modeled by Maxwell's equations and the relativistic Vlasov equation, in order to account for kinetic effects in the direction of the magnetic field. The dispersion relation of the waves is found and numerically solved. Results are qualitatively consistent with the fluid model in Ref. [10]:

the effective plasma frequency decreases, and the frequency range of the Alfvén branch is reduced, when the temperature is increased, so that electromagnetic waves propagate in a larger frequency range with respect to the cold case. Whereas for Alfvén waves the opposite occurs, being confined to a frequency range which is narrower than in the cold case.

However, quantitative results are different in both models. Regarding the electromagnetic branch, it is found that the effective plasma frequency is always larger in the kinetic model as compared with the fluid one. Thus, kinetic effects reduce the transparency of the plasma. As to the Alfvén branch, in both models it is found that the Alfvén speed decreases with temperature. In the fluid model, the Alfvén speed is zero for infinite temperature. However, in the kinetic case there is a critical, nonzero value of the temperature at which the Alfvén speed is zero. For temperatures above this critical value, the Alfvén branch is suppressed. The critical value depends on the background magnetic field. For larger values of the magnetic field, the critical value increases, and thus Alfvén waves can propagate for larger temperatures.

We also studied the fluid dispersion relation of the waves for nonzero drift, thus generalizing the numerical results in Ref. [10]. Besides, this analysis allowed us to study the dependence of the relativistic Lorentz factors on the drift, which was later used to study the kinetic model as detailed in Sec. V.

In this paper we considered kinetic effects in the direction of the background magnetic field only and did not study the effects of damping on the wave, either linear or nonlinear. Improvement along these lines, in order to include particle distribution functions depending on three-dimensional velocity, and to consider the effects of damping due to kinetic effects, will be dealt with in a future paper.

ACKNOWLEDGMENTS

This project has been financially supported by FONDECYT under Contracts No. 1110135 (J.A.V.), No. 1110729 (J.A.V.), No. 1080658 (V.M.), and No. 1121144 (V.M.). M.D. acknowledges financial support from CONICYT. We are also thankful for financial support by CEDENNA (J.A.V.). The authors also thank Felipe Asenjo for useful discussions.

-
- [1] G. Björnsson, M. A. Abramowicz, X. Chen, and J.-P. Lasota, *Astrophys. J.* **467**, 99 (1996).
 - [2] R. F. Sawyer, *Phys. Rev. D* **77**, 103011 (2008).
 - [3] J. F. C. Wardle, D. C. Homan, R. Ojha, and D. H. Roberts, *Nature (London)* **395**, 457 (1998).
 - [4] T. Tatsuno, V. I. Berezhiani, M. Pekker, and S. M. Mahajan, *Phys. Rev. E* **68**, 016409 (2003).
 - [5] T. Tajima and T. Taniuti, *Phys. Rev. A* **42**, 3587 (1990).
 - [6] M. F. Curtis, *The Theory of Neutron Stars Magnetospheres* (University of Chicago Press, Chicago, 1991).
 - [7] Y. N. Istomin and D. N. Sobyenin, *Astron. Lett.* **33**, 660 (2007).
 - [8] D. B. Blaschke, A. V. Prozorkevich, C. D. Roberts, S. M. Schmidt, and S. A. Smolyansky, *Phys. Rev. Lett.* **96**, 140402 (2006).
 - [9] H. Chen, *et al.* *High Energy Density Phys.* **7**, 225 (2011).
 - [10] F. A. Asenjo, V. Muñoz, J. A. Valdivia, and T. Hada, *Phys. Plasmas* **16**, 122108 (2009).
 - [11] S. M. Mahajan, *Phys. Rev. Lett.* **90**, 035001 (2003).
 - [12] A. R. Soto-Chavez, S. M. Mahajan, and R. D. Hazeltine, *Phys. Rev. E* **81**, 026403 (2010).
 - [13] J. Pino, H. Li, and S. Mahajan, *Phys. Plasmas* **17**, 112112 (2010).
 - [14] B. A. Bambah, S. M. Mahajan, and C. Mukku, *Phys. Rev. Lett.* **97**, 072301 (2006).
 - [15] V. Muñoz, *Phys. Plasmas* **11**, 3497 (2004).
 - [16] Y. Liu and S. Q. Liu, *Contrib. Plasma Phys.* **58**, 698 (2011).
 - [17] M. W. Verdon and D. B. Melrose, *Phys. Rev. E* **83**, 056407 (2011).
 - [18] R. Chaudhary, N. L. Tsintsadze, and P. K. Shukla, *J. Plasma Phys.* **76**, 875 (2010).
 - [19] R. Gill and J. S. Heyl, *Phys. Rev. E* **80**, 036407 (2009).
 - [20] V. Muñoz, T. Hada, and S. Matsukiyo, *Earth, Planets and Space* **58**, 1213 (2006).
 - [21] V. Muñoz and L. Gomberoff, *Phys. Plasmas* **9**, 2534 (2002).